A Frequency-Dependent Hybrid Implicit-Explicit FDTD Scheme for Dispersive Materials

Juan Chen and Anxue Zhang

School of Electronic and Information Engineering
Xi'an Jiaotong University, Xi'an 710049, China
anxuezhang@mail.xjtu.edu.cn

Abstract- A frequency-dependent hybrid implicit-explicit finite-difference time-domain (HIE-FDTD) method for dispersive materials is presented. This method has higher computation efficiency than the conventional FDTD method, because the time step in this method is only determined by two space discretizations. The accuracy of this method is demonstrated by computing the incident at a planar air-water interface over a wide frequency band including the effects of the frequency-dependent permittivity of water.

Index Terms- Dispersive materials, HIE-FDTD method, weakly conditional stability.

I. INTRODUCTION

The finite-difference time-domain (FDTD) method [1] has been proven to be an effective scheme that provides accurate predictions of field behaviors for varieties of electromagnetic interaction problems. However, as it is based on an explicit finite-difference algorithm, the Courant–Friedrich–Levy (CFL) condition [2] must be satisfied when this method is used. Therefore, a maximum time-step size is limited by the minimum cell size in a computational domain, which makes this method inefficient for the problems where fine scale structures are involved.

To overcome the CFL constraint on the time step size of the FDTD method, some unconditionally stable methods [3-7] and weakly conditionally stable [8-17] schemes have been studied, among which, the hybrid implicit-explicit finite-difference time-domain (HIE-FDTD) method, has been applied extensively [13-17]. In the HIE-FDTD method, the time step size is only determined by two space discretizations, which is useful for problems with very fine structures in one direction. The accuracy and computational efficiency of the HIE-FDTD method have been well validated in [13-15] and [17].

In this paper, the HIE-FDTD method will be extended to frequency-dependent materials. The formulations of HIE-FDTD for a frequency-dependent complex permittivity are presented and an example of calculation of a wave incident at a planar air-water interface over a wide frequency band is showed. The extension of the HIE-FDTD method to frequency-dependent permeability is similar.

II. FORMULATION

For this paper, we will assume that our materials are linear and isotropic, and only the permittivity is frequency-dependent. Extension to nonlinear or anisotropic dispersive materials should be possible.

The displacement vector D is related to the electric field E in the time domain by the following equation:

$$D(t) = \varepsilon_\infty \varepsilon_0 E(t) + \varepsilon_0 \int_0^t E(t-\tau)\chi(\tau)\, d\tau. \tag{1}$$

ε_0 is permittivity of free space, $\chi(\tau)$ is the electric susceptibility, and ε_∞ is the infinite frequency relative permittivity.

Using Yee's notation, we let $t = n\Delta t$ in (1), and each vector component of D and E can be written as:

$$D(t) \approx D(n\Delta t) = D^n = \varepsilon_\infty \varepsilon_0 E^n + \varepsilon_0 \int_0^{n\Delta t} E(n\Delta t - \tau)\chi(\tau) d\tau. \tag{2}$$

All field components are assumed to be constant over each time interval Δt. Therefore, we have, assuming $D(t)$ and $E(t)$ are zero for $t<0$:

$$D^n = \varepsilon_\infty \varepsilon_0 E^n + \varepsilon_0 \sum_{m=0}^{n-1} E^{n-m} \int_{m\Delta t}^{(m+1)\Delta t} \chi(\tau) d\tau. \tag{3}$$

$$D^{n+1} = \varepsilon_\infty \varepsilon_0 E^{n+1} + \varepsilon_0 \sum_{m=0}^{n} E^{n+1-m} \int_{m\Delta t}^{(m+1)\Delta t} \chi(\tau) d\tau. \tag{4}$$

When (3) is substituted in (4), we find:

$$\begin{aligned} D^{n+1} - D^n &= \varepsilon_\infty \varepsilon_0 \left[E^{n+1} - E^n \right] \\ &+ \varepsilon_0 E^{n+1} \int_0^{\Delta t} \chi(\tau) d\tau \\ &+ \varepsilon_0 \sum_{m=0}^{n-1} E^{n-m} \left\{ \begin{array}{l} \int_{(m+1)\Delta t}^{(m+2)\Delta t} \chi(\tau) d\tau \\ -\int_{m\Delta t}^{(m+1)\Delta t} \chi(\tau) d\tau \end{array} \right\}. \end{aligned} \tag{5}$$

For simplicity, we let:

$$\chi_m = \int_{m\Delta t}^{(m+1)\Delta t} \chi(\tau) d\tau. \tag{6}$$

$$\Delta\chi_m = \chi_m - \chi_{m+1}. \tag{7}$$

Then, we have:

$$\begin{aligned} E^{n+1} &= \frac{\varepsilon_\infty}{(\varepsilon_\infty + \chi_0)} E^n \\ &+ \frac{1}{(\varepsilon_\infty + \chi_0)} \sum_{m=0}^{n-1} E^{n-m} \Delta\chi_m \\ &+ \frac{D^{n+1} - D^n}{(\varepsilon_\infty \varepsilon_0 + \varepsilon_0 \chi_0)}. \end{aligned} \tag{8}$$

The three HIE-FDTD scalar equations that relate the components of the electric field E to the components of the magnetic field H can be readily obtained from (8) by using the discretized Maxwell-Ampere equation to replace $D^{n+1} - D^n$ in (8) with the curl of the H field,

$$\begin{aligned} E_y^{n+\frac{1}{2}}\left(i, j+\frac{1}{2}, k\right) &= \frac{\varepsilon_\infty}{(\varepsilon_\infty + \chi_0)} E_y^{n-\frac{1}{2}}\left(i, j+\frac{1}{2}, k\right) \\ &+ \frac{1}{(\varepsilon_\infty + \chi_0)} \sum_{m=0}^{n-\frac{3}{2}} E_y^{n-\frac{1}{2}-m}\left(i, j+\frac{1}{2}, k\right) \Delta\chi_m \\ &+ \frac{\Delta t}{(\varepsilon_\infty \varepsilon_0 + \varepsilon_0 \chi_0)\Delta z} \left[\begin{array}{l} H_x^n\left(i, j+\frac{1}{2}, k+\frac{1}{2}\right) \\ -H_x^n\left(i, j+\frac{1}{2}, k-\frac{1}{2}\right) \end{array} \right] \\ &- \frac{\Delta t}{(\varepsilon_\infty \varepsilon_0 + \varepsilon_0 \chi_0)\Delta x} \left[\begin{array}{l} H_z^n\left(i+\frac{1}{2}, j+\frac{1}{2}, k\right) \\ -H_z^n\left(i-\frac{1}{2}, j+\frac{1}{2}, k\right) \end{array} \right]. \end{aligned} \tag{9}$$

$$\begin{aligned} E_x^{n+1}\left(i+\frac{1}{2}, j, k\right) &= \frac{\varepsilon_\infty}{(\varepsilon_\infty + \chi_0)} E_x^n\left(i+\frac{1}{2}, j, k\right) \\ &+ \frac{1}{(\varepsilon_\infty + \chi_0)} \sum_{m=0}^{n-1} E_x^{n-m}\left(i+\frac{1}{2}, j, k\right) \Delta\chi_m \\ &- \frac{\Delta t}{(\varepsilon_\infty \varepsilon_0 + \varepsilon_0 \chi_0)} \frac{1}{\Delta z} \left[\begin{array}{l} H_y^{n+\frac{1}{2}}\left(i+\frac{1}{2}, j, k+\frac{1}{2}\right) \\ -H_y^{n+\frac{1}{2}}\left(i+\frac{1}{2}, j, k-\frac{1}{2}\right) \end{array} \right] \\ &+ \frac{\Delta t}{(\varepsilon_\infty \varepsilon_0 + \varepsilon_0 \chi_0)} \frac{1}{2\Delta y} \left[\begin{array}{l} H_z^{n+1}\left(i+\frac{1}{2}, j+\frac{1}{2}, k\right) \\ -H_z^{n+1}\left(i+\frac{1}{2}, j-\frac{1}{2}, k\right) \end{array} \right] \\ &+ \frac{\Delta t}{(\varepsilon_\infty \varepsilon_0 + \varepsilon_0 \chi_0)} \frac{1}{2\Delta y} \left[\begin{array}{l} H_z^{n}\left(i+\frac{1}{2}, j+\frac{1}{2}, k\right) \\ -H_z^{n}\left(i+\frac{1}{2}, j-\frac{1}{2}, k\right) \end{array} \right]. \end{aligned} \tag{10}$$

$$E_z^{n+1}\left(i,j,k+\frac{1}{2}\right)=\frac{\varepsilon_\infty}{\left(\varepsilon_\infty+\chi_0\right)}E_z^n\left(i,j,k+\frac{1}{2}\right)$$
$$+\frac{1}{\left(\varepsilon_\infty+\chi_0\right)}\sum_{m=0}^{n-1}E_z^{n-m}\left(i,j,k+\frac{1}{2}\right)\Delta\chi_m$$
$$+\frac{\Delta t}{\left(\varepsilon_\infty\varepsilon_0+\varepsilon_0\chi_0\right)\Delta x}\left[\begin{array}{l}H_y^{n+\frac{1}{2}}\left(i+\frac{1}{2},j,k+\frac{1}{2}\right)\\-H_y^{n+\frac{1}{2}}\left(i-\frac{1}{2},j,k+\frac{1}{2}\right)\end{array}\right]$$
$$-\frac{\Delta t}{2\left(\varepsilon_\infty\varepsilon_0+\varepsilon_0\chi_0\right)\Delta y}\left[\begin{array}{l}H_x^{n+1}\left(i,j+\frac{1}{2},k+\frac{1}{2}\right)\\-H_x^{n+1}\left(i,j-\frac{1}{2},k+\frac{1}{2}\right)\end{array}\right]$$
$$-\frac{\Delta t}{2\left(\varepsilon_\infty\varepsilon_0+\varepsilon_0\chi_0\right)\Delta y}\left[\begin{array}{l}H_x^{n}\left(i,j+\frac{1}{2},k+\frac{1}{2}\right)\\-H_x^{n}\left(i,j-\frac{1}{2},k+\frac{1}{2}\right)\end{array}\right].$$

(11)

It can be seen from these equations that the eqs. (10) and (11) can't be used for direct numerical calculation, because they all include the unknown components defined at the same time, thus, modified equations are derived from the original equations.

Updating of E_x^{n+1} component, as shown in eq. (10), needs the unknown H_z^{n+1} component at the same time. In the nonmagnetic media, the updating for H component is unchanged. The equation of the H_z^{n+1} component in the HIE-FDTD method is as follows:

$$H_z^{n+1}\left(i+\frac{1}{2},j+\frac{1}{2},k\right)=H_z^{n}\left(i+\frac{1}{2},j+\frac{1}{2},k\right)$$
$$+\frac{\Delta t}{2\mu\Delta y}\left[\begin{array}{l}E_x^{n+1}\left(i+\frac{1}{2},j+1,k\right)-E_x^{n+1}\left(i+\frac{1}{2},j,k\right)\\+E_x^{n}\left(i+\frac{1}{2},j+1,k\right)-E_x^{n}\left(i+\frac{1}{2},j,k\right)\end{array}\right]$$
$$-\frac{\Delta t}{\mu\Delta x}\left[E_y^{n+\frac{1}{2}}\left(i+1,j+\frac{1}{2},k\right)-E_y^{n+\frac{1}{2}}\left(i,j+\frac{1}{2},k\right)\right].$$

(12)

Thus, the E_x^{n+1} component has to be updated implicitly. Substituting eq. (12) into eq. (10), the equation for E_x^{n+1} field is given as,

$$\left[1+\frac{\Delta t^2}{2\varepsilon\mu\Delta y^2}\eta\right]E_x^{n+1}\left(i+\frac{1}{2},j,k\right)$$
$$-\frac{\Delta t^2}{4\varepsilon\mu\Delta y^2}\eta\left[E_x^{n+1}\left(i+\frac{1}{2},j+1,k\right)+E_x^{n+1}\left(i+\frac{1}{2},j-1,k\right)\right]$$
$$=\eta\varepsilon_\infty E_x^n\left(i+\frac{1}{2},j,k\right)+\eta\sum_{m=0}^{n-1}E_x^{n-m}\left(i+\frac{1}{2},j,k\right)\Delta\chi_m$$
$$+\eta\frac{\Delta t}{\varepsilon\Delta y}\left[H_z^n\left(i+\frac{1}{2},j+\frac{1}{2},k\right)-H_z^n\left(i+\frac{1}{2},j-\frac{1}{2},k\right)\right]$$
$$-\eta\frac{\Delta t^2}{2\mu\varepsilon\Delta x\Delta y}\left[E_y^{n+\frac{1}{2}}\left(i+1,j+\frac{1}{2},k\right)-E_y^{n+\frac{1}{2}}\left(i,j+\frac{1}{2},k\right)\right]$$
$$+\eta\frac{\Delta t^2}{2\mu\varepsilon\Delta x\Delta y}\left[E_y^{n+\frac{1}{2}}\left(i+1,j-\frac{1}{2},k\right)-E_y^{n+\frac{1}{2}}\left(i,j-\frac{1}{2},k\right)\right]$$
$$+\eta\frac{\Delta t^2}{4\varepsilon\mu\Delta y^2}\left[E_x^n\left(i+\frac{1}{2},j+1,k\right)-E_x^n\left(i+\frac{1}{2},j,k\right)\right]$$
$$+\eta\frac{\Delta t^2}{4\varepsilon\mu\Delta y^2}\left[E_x^n\left(i+\frac{1}{2},j-1,k\right)-E_x^n\left(i+\frac{1}{2},j,k\right)\right]$$
$$-\eta\frac{\Delta t}{\varepsilon\Delta z}\left[H_y^{n+\frac{1}{2}}\left(i+\frac{1}{2},j,k+\frac{1}{2}\right)-H_y^{n+\frac{1}{2}}\left(i+\frac{1}{2},j,k-\frac{1}{2}\right)\right].$$

(13)

here, $\eta=1/\left(\varepsilon_\infty+\chi_0\right)$.

The updating equation of E_z^{n+1} is similarly derived and calculated in the same way as eq.(13).

Note that if we assume the relative permittivity is independent of frequency, namely, $\chi(\tau)=0$, $\varepsilon_\infty=\varepsilon_r$, $\chi_m=0$ for all m, then, the above equations reduce to the standard HIE-FDTD formulations [13].

The above formulation is valid for electrically dispersive media. The extension to magnetically dispersive media would be similar.

In [15], the weakly conditional stability of the HIE-FDTD method is well validated. The time

step of the HIE-FDTD method is only determined by two spatial increments Δx and Δz, namely:

$$\Delta t \le 1 \Big/ \left(c\sqrt{\left(1/\Delta x\right)^2 + \left(1/\Delta z\right)^2} \right). \qquad (14)$$

$c = 1/\sqrt{\varepsilon\mu}$ is the speed of light in the medium. This is especially useful when the simulated structure has fine-scale dimensions in one direction, which will be validated in next section.

III. SIMULATION RESULTS

In order to demonstrate the validity and accuracy of the above formulation, a small current source above an incident at a planar air-water interface is presented here. The geometric configuration of the numerical simulation is shown in Fig.1. The dimensions of the perfect-electric-conductor box are 15cm $\times$15cm $\times$3cm. The box is filled with water up to height 7.5cm. A small current source applied along *y* direction is placed at the upper part of the box. The time dependence of the excitation function is:

$$g(t) = \exp[-4\pi(t - t_0)^2 / t_1^2], \qquad (15)$$

where t_0 and t_1 are constants, and both equal to 0.6×10^{-9}. The observation point B is set in the water, and 2 cm far from the source point A.

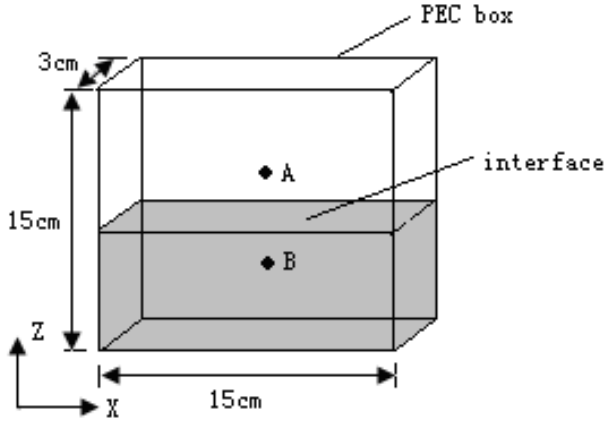

Fig. 1. Geometric configuration of the numerical simulation.

Applying the FDTD method to compute the time domain electric field component E_y at the observation point B, the cell size is chosen as $5\Delta y = \Delta x = \Delta z =$ 0.5cm, so that the computational domain is 30 $\times$30 $\times$30 cells. To satisfy the stability condition of the FDTD algorithm, the time-step size for conventional FDTD [18, 19] is $\Delta t \le$ 3.20ps. Here, the conventional FDTD is the FDTD method using recursive convolutional (RC) method to implement the dispersive media. For the HIE-FDTD scheme, the maximum time increment is only related to the space increments Δx and Δz, that is, $\Delta t \le$ 11.78ps. The HIE-FDTD method is using the recursive convolutional method with Debye model to implement the dispersive properties of the media.

For water, the complex permittivity $\varepsilon^*(\omega)$ can be described as

$$\varepsilon^*(\omega) = \varepsilon_0\left[\varepsilon_\infty + \left(\varepsilon_s - \varepsilon_\infty\right)/\left(1 + j\omega\tau_0\right)\right], \qquad (16)$$

where ε_s is the "static" permittivity, and τ_0 is the "relaxation time" constant. The water parameters used here are ε_s =81, ε_∞ =1.8, and $\tau_0 = 9.4\times10^{-12}$.

The summation (convolution) term of eq.(8) can be updated recursively by utilizing the equation (20) in [18], because the susceptibility function is an exponential. So, it doesn't require storing a large number of past time values E^n, and the computational time is saved. Only one additional number needs to be stored for each electric field component at each spatial index.

First, we validate the numerical stability condition (14). Figure 2 shows the electric field component E_y at observation point B calculated by using the HIE-FDTD methods with the time-step size Δt =11.78ps for a long time history. No instability problem is observed even for 5,000 steps, which validates the weakly conditional stability of the HIE-FDTD method numerically.

To demonstrate the high computational efficiency of HIE-FDTD method, we perform the numerical simulations for an 8 ns time history by using the conventional FDTD, and HIE-FDTD methods, and compare the CPU times taken by using these two methods. In the conventional FDTD method, the time-step size keeps a constant of 3.20 ps; while in the HIE-FDTD method, the time step size is 11.78ps.

Figure 3 shows the electric field component E_y at observation point B calculated by using the conventional FDTD and HIE-FDTD methods. It can be seen from this figure that the result calculated by the HIE-FDTD method agrees with

the result calculated by the conventional FDTD method. The HIE-FDTD method has almost the same accuracy as that of the conventional FDTD method. To validate this further, the divergence between these two methods are presented, as

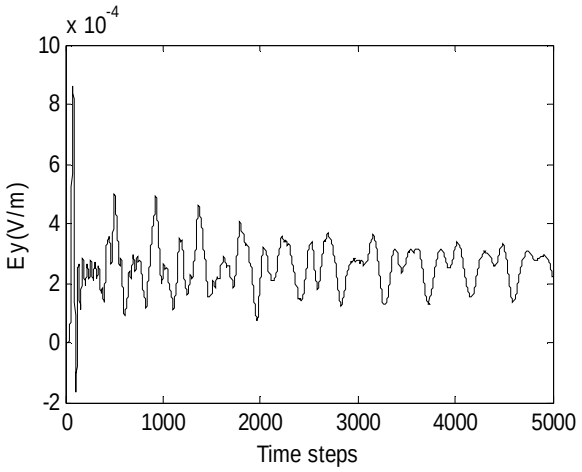

Fig. 2. The electric field component E_y at observation point B calculated by using the HIE-FDTD method with the time-step size Δt =11.78ps for a long time story.

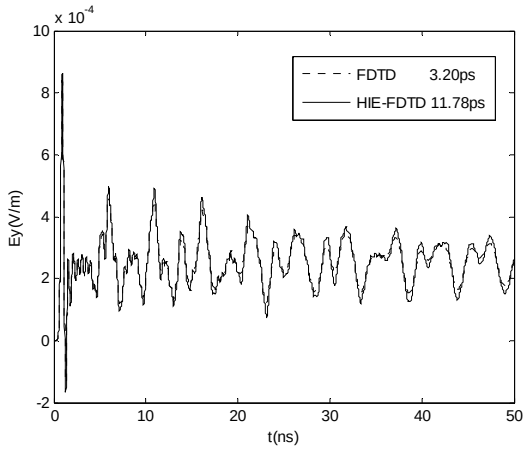

Fig. 3. The electric field component E_y at observation point B calculated by using the conventional FDTD (Δt =3.20ps), and HIE-FDTD methods (Δt =11.78ps).

shown in Fig.4. It can be seen from this figure that the error curve is limited and it doesn't increase as the addition of the computational time. It should be noted that the simulation takes 364 s for the conventional FDTD method and 121 s for the HIE-FDTD method. The time cost for the HIE-FDTD simulation is 1/3 times as that for the conventional FDTD simulation. So, we can conclude that the HIE-FDTD has higher efficiency than the conventional FDTD method, due to larger time step size used.

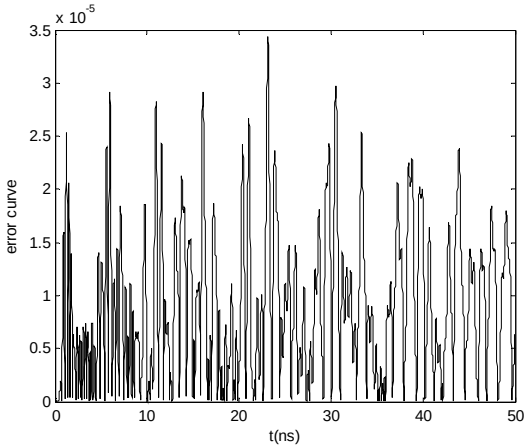

Fig. 4. The divergence between conventional FDTD (Δt =3.20ps), and HIE-FDTD methods (Δt =11.78ps).

IV. CONCLUSION

A frequency-dependent HIE-FDTD method for dispersive materials is presented. It is found that the technique is weakly conditionally stable and supports time steps greater than the CFL limit. A numerical example demonstrates that computation efficiency of the HIE-FDTD method is higher than the conventional FDTD method, and the accuracy of the HIE-FDTD is almost the same as that of the conventional FDTD method.

ACKNOWLEDGMENT

This work was supported by National Natural Science Foundations of China (No. 61001039 and 60501004), and also supported by the Research Fund for the Doctoral Program of Higher Education of China (20090201120030).

REFERENCES

[1] K. S. Yee, "Numerical Solution of Initial Boundary Value Problems Involving Maxwell's Equations in Isotropic Media," IEEE Trans. Antennas Propagat., vol. 14, pp. 302-307, May 1966.

[2] A. Taflove, *Computational Electrodynamics*,

Norwood, MA: Artech House, 1995.

[3] T. Namiki, "3-D ADI-FDTD method-unconditionally stable time-domain algorithm for solving full vector Maxwell's equations," IEEE Trans. Microw. Theory Tech., vol. 48, pp. 1743–1748, Oct. 2000.

[4] F. Zheng, Z. Chen, and J. Zhang, "A finite-difference time-domain method without the Courant stability conditions," IEEE Microw. Guided Wave Lett., vol. 9, pp. 441–443, Nov. 1999.

[5] G. Sun and C. W. Trueman, "Some fundamental characteristics of the one-dimensional alternate-direction-implicit finite-difference time-domain method," IEEE Trans. Microw. Theory Tech., vol. 52, pp. 46-52, Jan. 2004.

[6] S. G. García, T.-W. Lee, and S. C. Hagness, "On the accuracy of the ADI-FDTD method," IEEE Antennas Wireless Propag. Lett., vol. 1, pp. 31–34, 2002.

[7] I. Ahmed and Z. Chen, "Error reduced ADI-FDTD methods," IEEE Antennas Wireless Propagat. Lett., vol. 4, pp. 323-325, 2005.

[8] B. Huang, G. Wang, Y. S. Jiang, and W. B. Wang, "A hybrid implicit-explicit FDTD scheme with weakly conditional stability," Microwave Opt. Technol. Lett., vol. 39, pp. 97-101, Mar. 2003.

[9] J. Chen and J. G. Wang, "Weakly conditionally stability FDTD scheme with reduced split error," Electron. Lett., vol. 42, pp. 1017-1019, Aug. 2006.

[10] J. Chen and J. G. Wang, "3-D FDTD Method with Weakly Conditional Stability," Electron. Lett., vol. 43, pp. 2-3, Jan. 2007.

[11] J. Chen and J. Wang, "A novel WCS-FDTD method with weakly conditional stability," IEEE Trans. Electromagn. Compat., vol. 49, pp. 419-426, May 2007.

[12] J. Chen and J. Wang, "Using WCS-FDTD method to simulate various small aperture-coupled metallic enclosures," Microwave Opt. Technol. Lett., vol.49, pp. 1852-1858, Aug. 2007.

[13] J. Chen and J. Wang, "A 3-D hybrid implicit-explicit FDTD scheme with weakly conditional stability," Microw. Opt. Tech. Lett., vol. 48, pp. 2291-2294, Apr. 2006.

[14] J. Chen and J. Wang, "Comparison between HIE-FDTD method and ADI-FDTD method," Microw. Opt. Tech. Lett., vol. 49, pp. 1001-1005, 2007.

[15] J. Chen and J. Wang, "A three-dimensional semi-implicit FDTD scheme for calculation of shielding effectiveness of enclosure with thin slots," IEEE Trans. Electromagn. Compat., vol. 49, pp. 419-426, May. 2007.

[16] I. Ahmed and E. Li, "Conventional perfectly matched layer for weakly conditionally stable hybrid implicit and explicit-FDTD method," Microwave Opt. Technol. Lett., vol. 49, pp. 3106-3109, Dec. 2007.

[17] J. Chen and J. Wang, "Numerical simulation using HIE–FDTD method to estimate various antennas with fine scale structures," IEEE Trans. Antennas Propagat., vol. 55, pp. 3603-3612, Dec. 2007.

[18] R. Luebbers, F. P. Hunsberger, K. S. Kunz, R. B. Standler, and M. Schneider, "A frequency-dependent finite-difference time-domain formulation for dispersive materials," IEEE Trans. Electromagn. Compat., vol. 32, pp. 222-227, Aug.1990.

[19] J. H. Beggs, "Validation and demonstration of frequency approximation methods for modeling dispersive media in FDTD," Appl. Comput. Electronm., vol. 14, pp. 52-58, Feb.1999.